Metal-insulator transition in the spinel-type Cu(Ir1-xVx)2S4

Metal-insulator transition in the spinel-type Cu(Ir1-xVx)2S4

doi: info:doi/10.1016/j.physb.2006.04.006

Metal-insulator transition in the spinel-type $Cu(Ir_{1-x}V_x)_2S_4$

Y. Kawashima, N. Horibe, J. Awaka, H. Yamamoto,

S. Ebisu, and S. Nagata*

Department of Materials Science and Engineering, Muroran Institute of Technology,

27-1 Mizumoto-cho, Muroran, Hokkaido 050-8585, Japan

Abstract

The spinel $CuIr_2S_4$ exhibits a temperature-induced metal-insulator (*M-I*) transition at around T_{M-I} = 226 K with a structural transformation, at which a simultaneous bond-dimerization with spin-singlet state and charge-ordering transition takes place. Conversely, CuV_2S_4 exhibits two step anomalies at about 92 K and 56 K, reflecting the *CDW* state. High-purity spinel-type $Cu(Ir_{1-x}V_x)_2S_4$ specimens have been synthesized. The lattice constant does not obey Vegard's law, but looks like a parabolic curve. The *d*-electrons on the octahedral B-sites play a dominant role in determining the physical properties. A low substitution ($x \approx 0.04$) of V for Ir leads to disappearance of the step-like sharp *M-I* transition, and vice versa, a low substitution of Ir for V destroys the *CDW* transition. The local structural and orbital degrees of freedom in $Cu(Ir_{1-x}V_x)_2S_4$ couple to the spin system and the electronic state. The *M-I* transition and the *CDW* state are incompatible with each other in $Cu(Ir_{1-x}V_x)_2S_4$. In the metallic phase, a novel relationship, namely "a mirror image effect" has been manifestly found between the residual resistivity and the electronic energy density-of-states $D(\varepsilon_F)$ at the Fermi level. The lower is the resistivity, the higher is the value of $D(\varepsilon_F)$. Furthermore, a composition-induced gradual *M-I* transition is found over the range of $0.00 \leq x \leq 1.00$, where the most insulating behavior is displayed around $x \approx 0.2$~0.3.

PACS：71.30.+h, 75.50.-y, 72.80.Ga
keywords: Spinel-type $CuIr_2S_4$; CuV_2S_4; $Cu(Ir_{1-x}V_x)_2S_4$; Metal-insulator transition; Electrical conductivity; Magnetic properties

*Corresponding author.
Fax : +81-143-46-5612. *E-mail address* : naga-sho@mmm.muroran-it.ac.jp (S. Nagata)

1. Introduction

The thiospinel compound $CuIr_2S_4$ has spinel structure at room temperature where Cu ions occupy the A (tetrahedral) site and Ir ions occupy the B (octahedral) site, as shown in Fig. 1. $CuIr_2S_4$ exhibits a metal-insulator (*M-I*) transition at around T_{M-I} = 226 K with structural transformation, showing hysteresis on heating and cooling. The resistivity of $CuIr_2S_4$ varies abruptly by nearly a factor 300 at T_{M-I} [1-69]. The striking feature is the absence of localized magnetic moment below T_{M-I}. A comprehensive review of this *M-I* transition is provided in ref [67]. Recently, orbital induced Peierls state concerned with the origin of *M-I* transition in $CuIr_2S_4$ has been investigated in detail using X-ray photoemission spectroscopy (*XPS*) [68, 69].

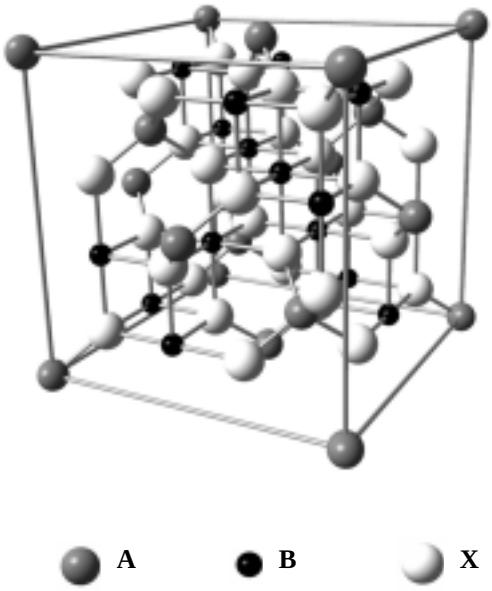

Fig. 1. The cubic unit cell of the spinel structure. Cu ions occupy the A (tetrahedral) sites, and Ir and V ions occupy the B (octahedral) sites. Large white circles indicate S ions.

On the other hand, CuV_2S_4 has the same spinel structure and shows two-step anomalies at about 92 K and 56 K, in the resistivity and in the magnetic susceptibility [70-83]. These anomalies are related to a charge density wave (*CDW*) state. The observation of *CDW* in only a very few three-dimensional cubic structure makes CuV_2S_4 notable, so intensive investigations have been carried out. The recent work reported that the two-step transitions came from the structural modulations and Fermi-liquid behavior for strongly correlated electrons was observed at low temperatures [81].

This paper will present the variation of the *M-I* transition in $CuIr_2S_4$ and the change of the anomalies in CuV_2S_4 in the substituted system $Cu(Ir_{1-x}V_x)_2S_4$. We have successfully synthesized high-quality specimens of $Cu(Ir_{1-x}V_x)_2S_4$. Systematical study of structural, electrical, and magnetic properties has been made. The variation in the *M-I* transition with V composition x is examined. The sharp step-like transition varies drastically with x and disappears around $Cu(Ir_{0.96}V_{0.04})_2S_4$. The transition temperature T_{M-I} is fairly sensitive to the value of x. Conversely, the two-step anomaly of CuV_2S_4 becomes ill defined, because the resistivity and the susceptibility jumps are not clear at around the composition $Cu(Ir_{0.02}V_{0.98})_2S_4$ and disappear completely around $Cu(Ir_{0.05}V_{0.95})_2S_4$. A basic characteristic of the phase diagram of temperature vs. composition x is provided experimentally for $Cu(Ir_{1-x}V_x)_2S_4$ system. The *M-I* transition and the *CDW* state are strictly incompatible with each other in $Cu(Ir_{1-x}V_x)_2S_4$.

2. Experimental methods

The polycrystalline specimens were prepared by a solid-state reaction. Mixtures of high-purity fine powders of Cu (purity 99.99 %, melting point 1357.5 K), Ir (99.99 %, 2716 K), V (99.9 %, 2190 K), and S (99.999 %, 385.8 K) with normal stoichiometry were heated in sealed quartz tubes to 1123 K and kept at this temperature for 10 days. The resultant powder specimens were reground and pressed to rectangular bars and then were heated to 1123 K for 2 days.

The identification of the crystal structure and the determination of the lattice constants were carried out by X-ray powder diffraction using CuKα radiation at room temperature. The resistivity ρ of sintered specimens with dimensions of about $2\times2\times10\,mm^3$ was measured by a standard DC four-probe method over the temperature range 4.2 K to room temperature. The DC magnetic susceptibility χ of powder specimens was measured with a Quantum Design superconducting quantum interference device (*rf*-SQUID) magnetometer over the temperature range 4.2-300 K at intervals of 5.0 K in an applied magnetic field of 10.000 kOe.

3. Results and discussion

3.1. *Lattice constant of* $Cu(Ir_{1-x}V_x)_2S_4$

Powder X-ray diffraction patterns at room temperature confirm that $Cu(Ir_{1-x}V_x)_2S_4$ has the spinel type structure in all the V-composition range. Representative results of the X-ray diffraction patterns are presented in Fig. 2. The indices, the *d* spacings, and the intensities are listed in Tables 1 to 3. The lattice constant, *a*, obtained by the least square method, varies as shown in Fig. 3 at room temperature. The composition dependence of the lattice constant *a* does not obey the Vegard's law, but looks like a parabolic curve. The values of *a* are listed in Table 4, *a* decreases with V substitution to a broad minimum at around $x = 0.55$; then from $x = 0.55$ to $x = 1.00$ *a* increases smoothly. The ionic radius of V (0.65 Å for V^{3+}) is slightly smaller than that of Ir (0.66 Å for Ir^{3+}) for the same valence. A similar behavior of the variation of the lattice constant *a* with composition, has been observed in the $Cu(Ir_{1-x}Ti_x)_2S_4$ system by Nagata *et al*. [51] and in the $Cu(Ir_{1-x}Cr_x)_2S_4$ system by Endoh *et al*. [57]. A reasonable interpretation of the parabolic curve for the lattice constant in Fig. 3 has been proposed by previous researchers [51, 57]. Two effects can be superimposed: the first effect is that the ionic radius decreases with *x* obeying the Vegard's law, the second one is the influence originating from the cohesive energy of the conduction electrons in the electron *d*-band. The latter effect is caused by the delocalized nature of *d* electrons in $Cu(Ir_{1-x}V_x)_2S_4$. Presumably, the influence the second effect is much stronger than that of the former one. Here it should be pointed out that the characteristic parabolic curve can be found manifestly only in special circumstances, where the number of *d* electron of the substituting atoms on the B-site is much different from that of an Ir atom, such as in the $Cu(Ir_{1-x}M_x)_2S_4$ (M = Ti, V, and Cr) systems. The variation of the lattice constant as indicated in Fig. 3 may influence the electrical and magnetic properties.

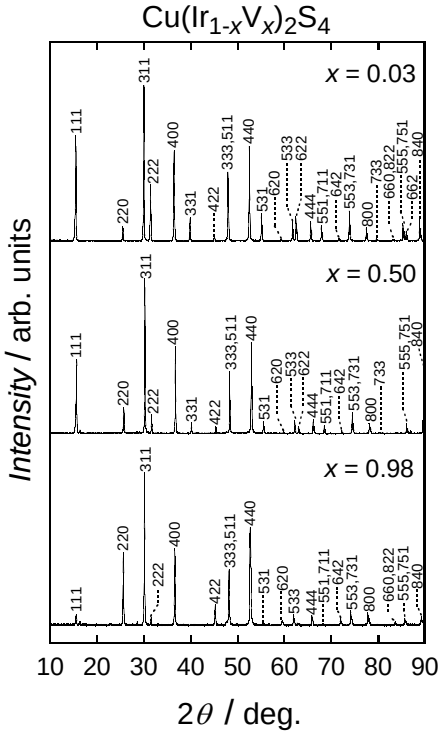

Fig. 2. Powder X-ray diffraction patterns for x = 0.03, 0.50 and 0.98 at room temperature.

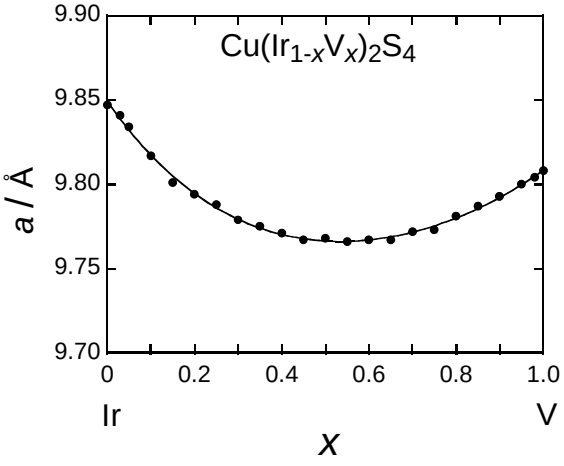

Fig. 3. The lattice constant a as a function of V composition x at room temperature.

Table 1. Indices, observed and calculated values of d spacings and observed intensities for $Cu(Ir_{1-x}V_x)_2S_4$, x = 0.03 with lattice constant a = 9.841 Å

h	k	l	d_{obs}(Å)	d_{cal}(Å)	I_{obs}
1	1	1	5.7048	5.6817	58
2	2	0	3.4848	3.4793	9
3	1	1	2.9723	2.9672	100
2	2	2	2.8448	2.8409	36
4	0	0	2.4636	2.4603	62
3	3	1	2.2597	2.2577	16
4	2	2	2.0103	2.0088	3
3	3	3	1.8953	1.8939	50
5	1	1		1.8939	
4	4	0	1.7410	1.7397	69
5	3	1	1.6643	1.6634	20
6	2	0	1.5571	1.5560	1
5	3	3	1.5017	1.5007	15
6	2	2	1.4844	1.4836	18
4	4	4	1.4212	1.4204	15
5	5	1	1.3786	1.3780	12
7	1	1		1.3780	
6	4	2	1.3155	1.3151	2
5	5	3	1.2817	1.2812	23
7	3	1		1.2812	
8	0	0	1.2306	1.2301	10
7	3	3	1.2026	1.2023	1
6	6	0	1.1602	1.1598	1
8	2	2		1.1598	
5	5	5	1.1367	1.1363	13
7	5	1		1.1363	
6	6	2	1.1292	1.1288	7
8	4	0	1.1005	1.1003	17

Table 2. Indices, observed and calculated values of d spacings and observed intensities for $Cu(Ir_{1-x}V_x)_2S_4$, x = 0.50 with lattice constant a = 9.768 Å

h	k	l	d_{obs}(Å)	d_{cal}(Å)	I_{obs}
1	1	1	5.6541	5.6396	40
2	2	0	3.4582	3.4535	16
3	1	1	2.9492	2.9452	100
2	2	2	2.8220	2.8198	13
4	0	0	2.4442	2.4420	59
3	3	1	2.2425	2.2409	8
4	2	2	1.9952	1.9939	5
3	3	3	1.8813	1.8799	45
5	1	1		1.8799	
4	4	0	1.7275	1.7268	69
5	3	1	1.6521	1.6511	9
6	2	0	1.5448	1.5445	1
5	3	3	1.4904	1.4896	10
6	2	2	1.4734	1.4726	5
4	4	4	1.4105	1.4099	11
5	5	1	1.3683	1.3678	6
7	3	1		1.3678	
6	4	2	1.3058	1.3053	2
5	5	3	1.2720	1.2717	15
7	3	1		1.2717	
8	0	0	1.2214	1.2210	8
7	3	3	1.1936	1.1934	1
5	5	5	1.1282	1.1279	6
7	3	1		1.1279	
8	4	0	1.0924	1.0921	5

Table 3. Indices, observed and calculated values of d spacings and observed intensities for $Cu(Ir_{1-x}V_x)_2S_4$, $x = 0.98$ with lattice constant $a = 9.805$ Å

h	k	l	d_{obs}(Å)	d_{cal}(Å)	I_{obs}
1	1	1	5.6757	5.6609	6
2	2	0	3.4715	3.4666	47
3	1	1	2.9607	2.9563	100
2	2	2	2.8342	2.8305	5
4	0	0	2.4545	2.4513	54
4	2	2	2.0027	2.0014	16
3	3	3	1.8878	1.8870	43
5	1	1		1.8870	
4	4	0	1.7342	1.7333	75
5	3	1	1.6560	1.6573	1
6	2	0	1.5514	1.5503	4
5	3	3	1.4960	1.4952	9
6	2	2	1.4788	1.4782	2
4	4	4	1.4158	1.4152	7
5	5	1	1.3732	1.3730	1
7	1	1		1.3730	
6	4	2	1.3105	1.3102	5
5	5	3	1.2767	1.2765	11
7	3	1		1.2765	
8	0	0	1.2258	1.2256	9
8	2	2	1.1559	1.1555	2
5	5	5	1.1324	1.1322	5
7	5	1		1.1322	
8	4	0	1.0964	1.0962	6

Table 4. Lattice constant a of spinel-type $Cu(Ir_{1-x}V_x)_2S_4$ at room temperature.

x	a (Å)
0.00	9.847
0.03	9.841
0.05	9.834
0.10	9.817
0.15	9.801
0.20	9.794
0.25	9.788
0.30	9.779
0.35	9.775
0.40	9.771
0.45	9.767
0.50	9.768
0.55	9.766
0.60	9.767
0.65	9.767
0.70	9.772
0.75	9.773
0.80	9.781
0.85	9.787
0.90	9.793
0.95	9.800
0.98	9.805
1.00	9.808

3.2. *Variation of the metal-insulator and CDW transitions in* $Cu(Ir_{1-x}V_x)_2S_4$

Fig. 4 shows the temperature dependence of the electrical resistivity for the sintered specimens. With increasing V-composition x, T_{M-I} decreases steeply and the height of the resistivity jump at T_{M-I} becomes smaller as shown in Fig. 5. The temperature dependence of the resistivity below T_{M-I} is semiconductive. The resistivity jump becomes ill defined around $x = 0.05$. With increasing x over $x = 0.30$, the resistivity becomes lower and the metallic state is recovered at still higher compositions. Figs. 5 and 6 present the results for the region $0.00 \leq x \leq 0.10$ and $0.90 \leq x \leq 1.00$, respectively.

Pure CuV_2S_4 shows strong sample dependence of the resistivity so far [70-83]. Recently the results of the resistivity for CuV_2S_4 converge on the representative datum by H. Okada *et al.* [81]. The single crystals of CuV_2S_4 are not always of high purity and high quality [74, 82-83].

Fig. 7 shows the temperature dependence of the magnetic susceptibility χ for the powder specimens. The value of χ is defined as $\chi = M / H$: the magnetization M divided by the applied magnetic field H. Measurements were carried out at a constant applied magnetic field of 10 kOe. Figs. 8 to 10 present the results for the V-composition region of $0.00 \leq x \leq 0.15$, $0.20 \leq x \leq 0.70$ and the higher x region of $0.90 \leq x \leq 1.00$. The resistivity jump due to the T_{M-I} corresponds exactly to the step-like anomaly of the susceptibility for $x = 0.00$ and 0.03. For $x \geq 0.05$, no step-like anomaly is observed. With increasing V-composition x, the temperature dependence of the susceptibility becomes rather steeper below T_{M-I} as seen in Fig. 8. It should be noticed that the magnetic susceptibility of $CuIr_2S_4$, in the low

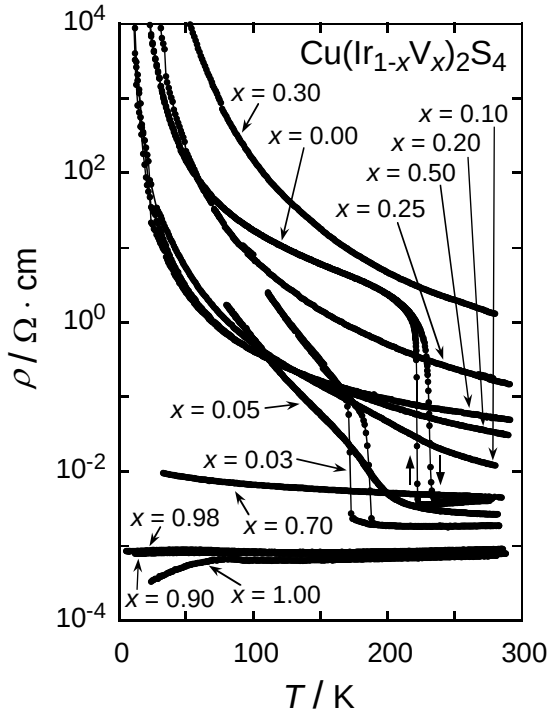

Fig. 4. Temperature dependence of the electrical resistivity ρ for sintered $Cu(Ir_{1-x}V_x)_2S_4$ specimens.

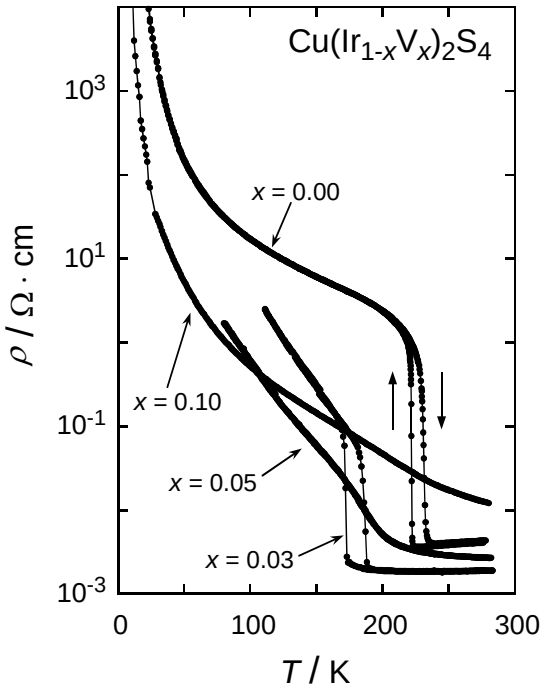

Fig. 5. Temperature dependence of the electrical resistivity ρ for sintered $Cu(Ir_{1-x}V_x)_2S_4$ specimens for $0.00 \leq x \leq 0.10$.

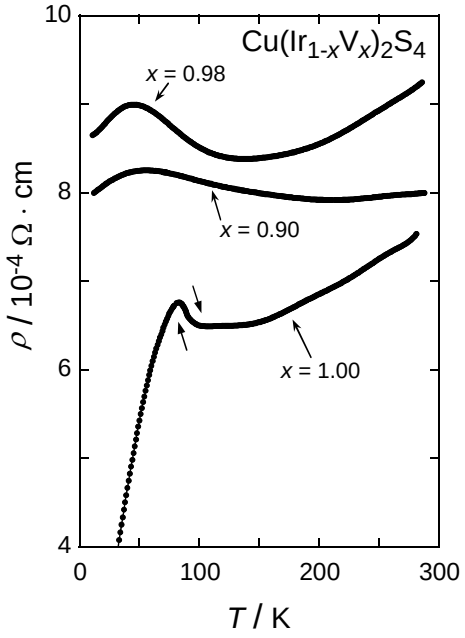

Fig. 6. Temperature dependence of the electrical resistivity ρ for sintered $Cu(Ir_{1-x}V_x)_2S_4$ specimens for $0.90 \leq x \leq 1.00$.

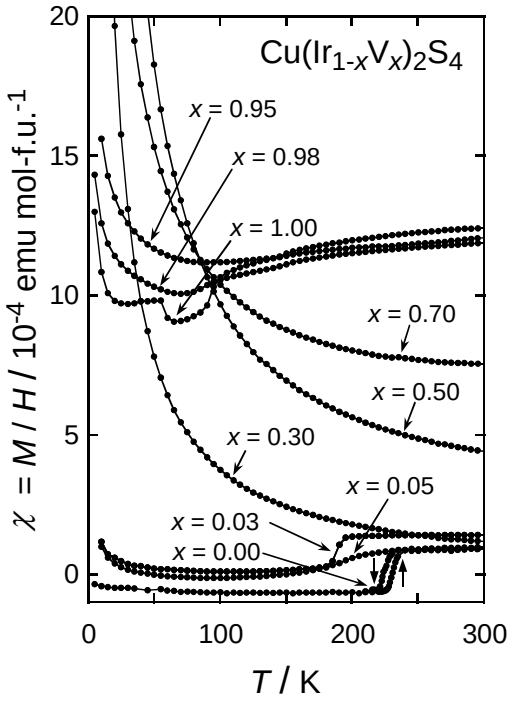

Fig. 7. Magnetic susceptibility versus temperature of $Cu(Ir_{1-x}V_x)_2S_4$. The applied magnetic field is 10 kOe.

temperature insulating phase, indicates basically a non-magnetic state except a paramagnetic behavior and small amount of diamagnetism due to the core atomic orbitals. Fig. 9 shows the paramagnetic behavior with temperature-independent constant value χ_0 which is defined in the next section.

The susceptibility of CuV_2S_4 (x = 1.00) exhibits two step anomalies around T = 90 K and 55 K due to the *CDW* transition, as can be seen in Fig 10. The absolute value of the susceptibility for CuV_2S_4 and the general feature of the temperature dependence with the two-step anomaly are in agreement with the result of the previous researchers [81]. With x decreasing a little below x = 1.00, the *CDW* transition becomes ill defined. For x = 0.98, no step-like anomaly is observed at 55 K and the sharp jump smears out around 90 K. The sharp anomaly disappears beyond the extremely little substitution of Ir atom for V.

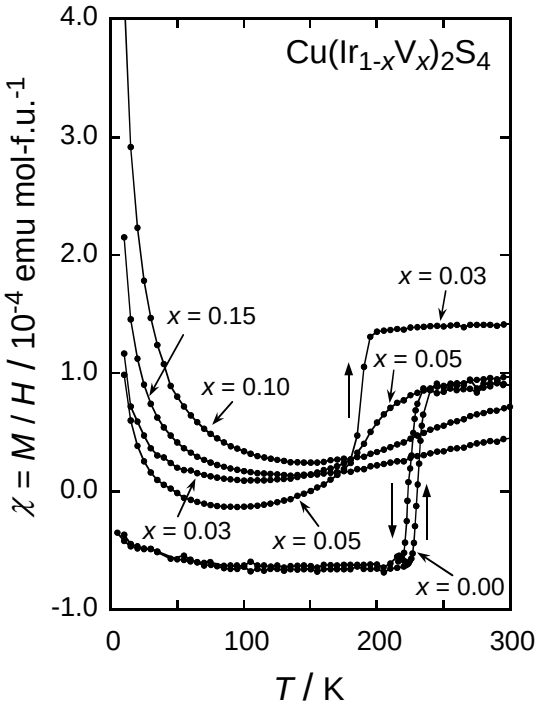

Fig. 8. Temperature dependence of the electrical resistivity ρ for sintered $Cu(Ir_{1-x}V_x)_2S_4$ specimens for $0.90 \leq x \leq 1.00$.

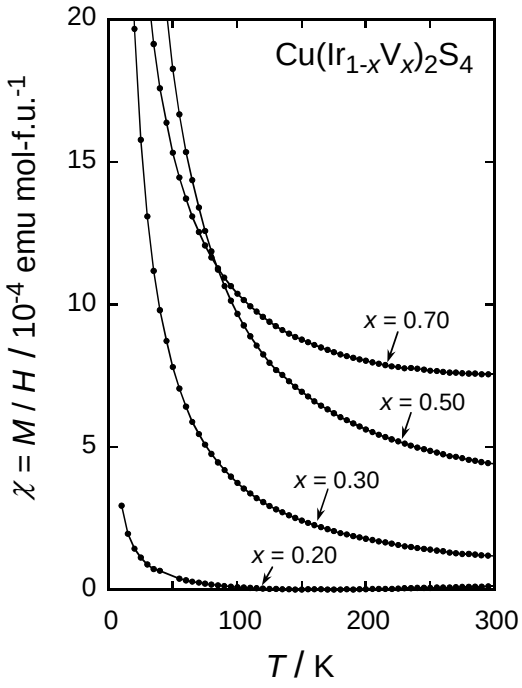

Fig. 9. Temperature dependence of the electrical resistivity ρ for sintered $Cu(Ir_{1-x}V_x)_2S_4$ specimens for $0.90 \leq x \leq 1.00$.

3.3. *The value of effective magnetic moment*

The magnetic susceptibility can be fitted to a modified Curie-Weiss law, $\chi = C / (T - \theta) + \chi_0$ where χ_0 is the temperature independent term, C the Curie constant, and θ the Weiss temperature. Table 5 provides the summary of the magnetic data. The second column from the right in Table 5 indicates the value calculated assuming that only the V ions possess a magnetic moment. It is hard to draw the definite conclusion that the induced magnetic moment originates from the substitution of Ir by V. The effective magnetic moment per V ion in the low temperature region is much less than the value corresponding to s = 1/2, leading to $\sqrt{s(s+1)}$ =1.73. There is no indication of any systematic variation of the effective magnetic moment. Therefore, there seems to be no intrinsic localized magnetic moment in this system. The low temperature increase in the susceptibility may arise from the existence of extrinsic localized moments at impurity sites or at other kind of lattice imperfections due to e.g. nonstoichiometry.

Table 5. Summary of the magnetic properties of $Cu(Ir_{1-x}V_x)_2S_4$. These numerical values are extracted from the magnetic susceptibility at lower temperatures based on the modified Curie-Weiss law $\chi = C / (T - \theta) + \chi_0$. The value of χ_0 includes appreciable experimental errors.

x	χ_0 (emu mol^{-1})	C (emu K mol-f.u.$^{-1}$)	θ (K)	p_{eff} (f.u.$^{-1}$)	p_{eff} (V-ion^{-1})	Temperature (K)
0.03	-7.28×10^{-6}	1.47×10^{-3}	-2.541	0.108	0.443	10 - 50
0.05	2.77×10^{-5}	1.34×10^{-3}	-0.429	0.103	0.327	10 - 50
0.10	-1.45×10^{-5}	4.78×10^{-3}	-0.598	0.195	0.437	4.2 - 100
0.15	-1.17×10^{-5}	2.80×10^{-3}	-2.506	0.150	0.273	10 - 50
0.20	-2.78×10^{-5}	3.66×10^{-3}	-1.241	0.171	0.270	10 - 100
0.30	-5.90×10^{-5}	3.59×10^{-2}	5.420	0.535	0.691	55 - 300
0.50	1.90×10^{-4}	7.30×10^{-2}	4.380	0.764	0.764	55 - 300
0.70	5.83×10^{-4}	4.19×10^{-2}	7.493	0.579	0.489	55 - 200
0.90	1.01×10^{-3}	1.28×10^{-2}	-6.354	0.320	0.238	4.5 - 100
0.95	9.95×10^{-4}	9.96×10^{-3}	-7.853	0.282	0.205	10 - 50
0.98	9.15×10^{-4}	6.85×10^{-3}	-9.549	0.234	0.167	10 - 65

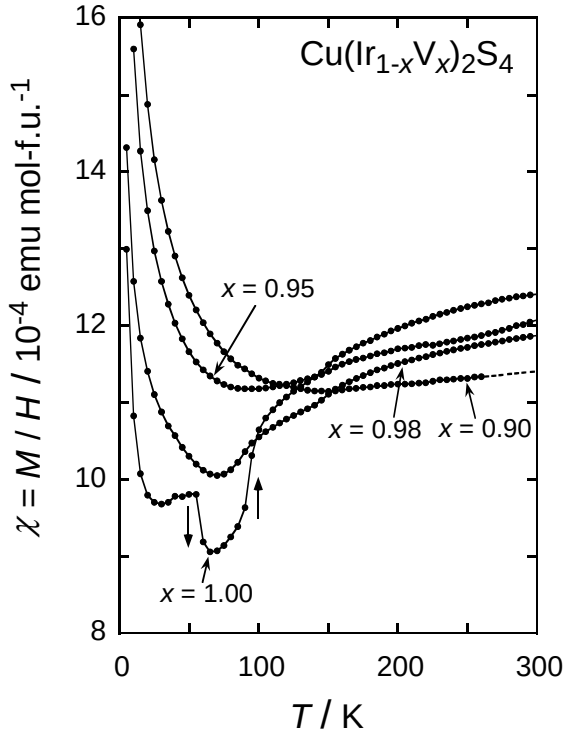

Fig. 10. Magnetic susceptibility versus temperature of $Cu(Ir_{1-x}V_x)_2S_4$ for $0.90 \leq x \leq 1.00$. The applied magnetic field is 10 kOe.

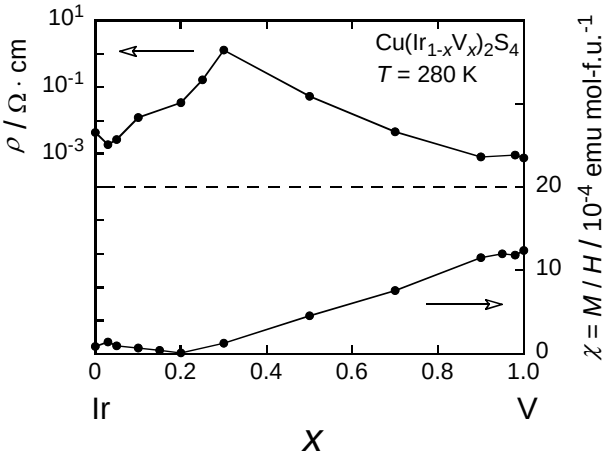

Fig. 11. Comparison of the resistivity and the magnetic susceptibility at 280 K for $0.00 \leq x \leq 1.00$.

3.4. *A mirror image effect between the residual resistivity and the Pauli susceptibility*

Fig. 11 presents the composition dependence of the resistivity and the magnetic susceptibility at 280 K. Below 230 K, the *M-I* transition occurs for low values of x, moreover the Curie like behavior arises for all the compositions x. Therefore it is hard to extract the metallic property. Indeed, for the composition region $x \geq 0.10$, the metallic state is not verified from the temperature dependence of the resistivity. Nevertheless, Fig. 11 gives a rough sketch of the general relation between the magnitude of the residual resistivity and the Pauli paramagnetic contribution. The Pauli paramagnetic susceptibility is proportional to the electronic energy density-of-states at the Fermi level, $D(\varepsilon_F)$. The measured susceptibility, shown in Fig. 11, lower panel, has a minimum value at around x = 0.20, and shows two approximately linear parts, with opposite signs.

Figs. 12 and 13 indicate the expanded plots for the composition dependences of the resistivity and the susceptibility at 280 K for $0.00 \leq x \leq 0.20$ and $0.70 \leq x \leq 1.00$, respectively. It should be noted that the susceptibility corresponds inversely to the height of resistivity, say, "a mirror image effect" or "an alligator mouth". This mirror image effect between the residual resistivity and $D(\varepsilon_F)$ can be clearly seen in Figs. 12 and 13: the lower is the resistivity, the higher is the value of $D(\varepsilon_F)$.

Almost the same effect has been observed and reported in detail for the $Cu(Ir_{1-x}Pt_x)_2S_4$ system by Matsumoto *et al.* [41] and also for the $Cu(Ir_{1-x}Ti_x)_2S_4$ system by Nagata *et al.* [51]. Over the range of $0.20 \leq x \leq 0.70$, the metallic state at 280 K is not confirmed. Consequently, the precise comparison itself does not make sense for the results of Fig. 11, although the mirror effect is present for $x > 0.3$.

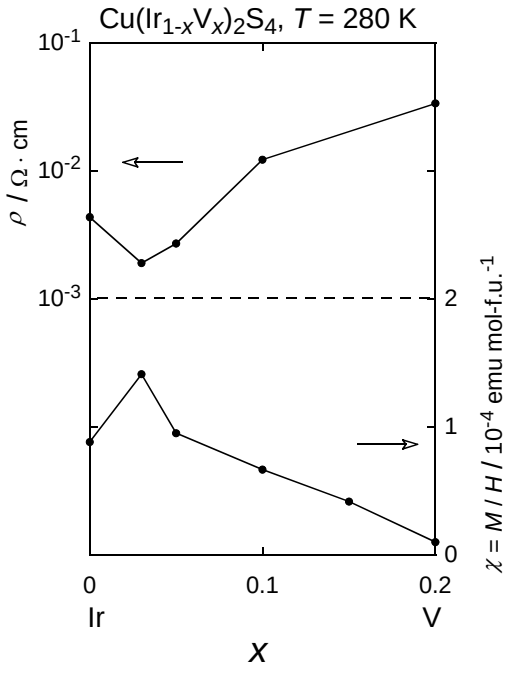

Fig. 12. Comparison of the resistivity and the magnetic susceptibility at 280 K for $0.00 \leq x \leq 0.20$.

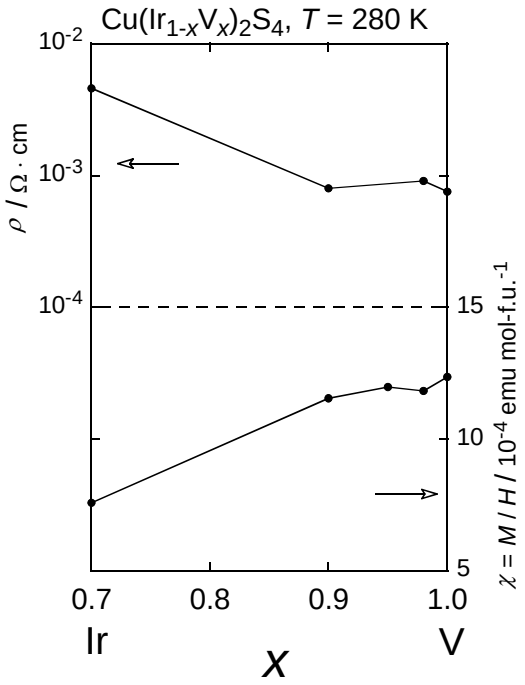

Fig. 13. Comparison of the resistivity and the magnetic susceptibility at 280 K for $0.70 \leq x \leq 1.00$.

3.5. *Phase diagram of* $Cu(Ir_{1-x}V_x)_2S_4$

Fig. 14 shows a crude sketch of a phase diagram for T versus x, which displays only an extremely low composition region ($x \leq 0.10$) and a high one ($x \geq 0.98$) in the $Cu(Ir_{1-x}V_x)_2S_4$ system. The *M-I* transition and the *CDW* state are incompatible with each other in $Cu(Ir_{1-x}V_x)_2S_4$. The temperature induced sharp *M-I* transition is seen for $x \leq 0.03$ and is smeared at around $x = 0.05$. The shaded area of $0.03 \; x \leq 0.05$ shows a weak indication of the *M-I* transition. With increasing x, the temperature dependence of the resistivity changes from metallic to semiconducting. Weakly doped $CuIr_2S_4$ can lie on either side of the *M-I* transition induced by electron correlation. Furthermore, a composition induced gradual *M-I* transition is found over the range of $0.00 \leq x \leq 1.00$, where the more insulating behavior is found around the composition region of $x \approx 0.2$~0.3.

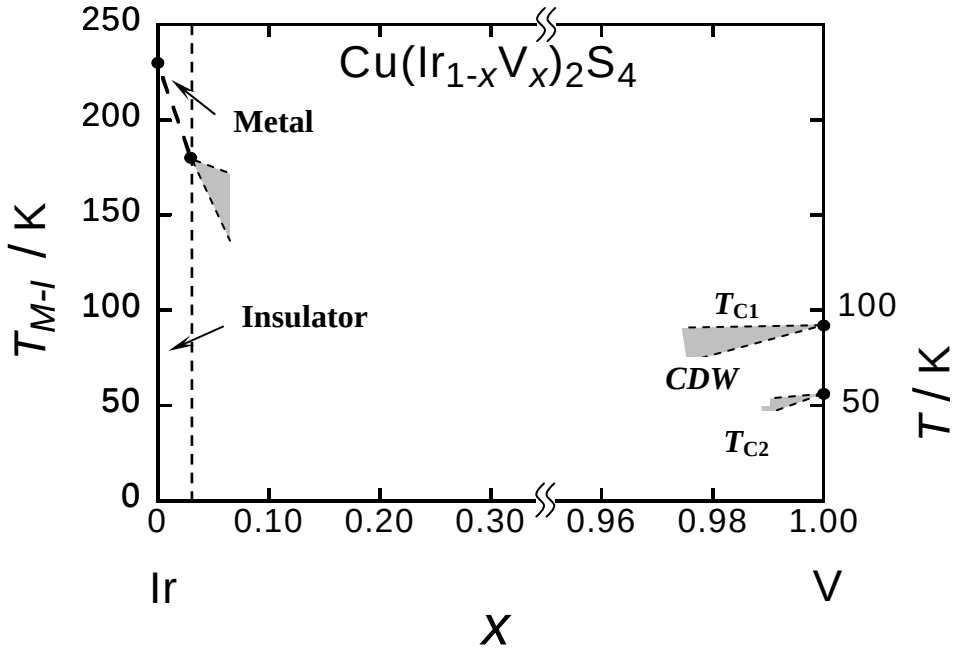

Fig. 14. A phase diagram of $Cu(Ir_{1-x}V_x)_2S_4$ for temperature versus composition x. For $x \leq 0.03$, solid circles indicate the *M-I* transition temperature T_{M-I}. For $x = 1.00$, a two- step *CDW* transition is observed. The sharp *M-I* transition in $CuIr_2S_4$ and the step-like *CDW* transition in CuV_2S_4 disappear easily with an extremely low substitution. The *M-I* transition and the *CDW* state are incompatible with each other in $Cu(Ir_{1-x}V_x)_2S_4$, see text.

Solid circles for $x = 1.00$ show a two-step transition at T_{C1} and T_{C2}. The discovery of the *CDW* transition in the cubic spinel CuV_2S_4 has attracted intensive researches [70]. In contradistinction to this trend, a recent study indicates a two-step structural modulation and Fermi liquid behavior [81]. The transition at T_{C1} (92 K) is reversible from cubic to tetragonal, while the transition at T_{C2} (56 K) exhibits a thermal hysteresis at which the lattice constant is modulated, a discontinuity without changing the symmetry [81]. The origin of the two anomalies in CuV_2S_4 may remain controversial, but is not the main subject in the present study. Here, we refer to the two-step transitions T_{C1} and T_{C2} as *CDW* transitions. The sharp two-step transitions are smeared out at around $x = 0.98$. The shaded areas, for the range of $0.97 \leq x \leq 1.00$, show weak indications of T_{C1} and T_{C2}. Extensive theoretical effort to understand the present experimental results is required.

Acknowledgments

The authors would like to thank Dr. Ryo Endoh and Mr. S. Ito for their valuable help with the measurements. The present work was supported financially by the Asahi Glass Foundation (H17-2, 2005, Tokyo).

References

[1] S. Nagata, T. Hagino, Y. Seki, T. Bitoh, Physica B 194-196 (1994) 1077.

[2] T. Furubayashi, T. Matsumoto, T. Hagino, S. Nagata, J. Phys. Soc. Jpn. 63 (1994) 3333.

[3] T. Hagino, Y. Seki, S. Nagata, Physica C 235-240 (1994) 1303.

[4] T. Hagino, T. Tojo, T. Atake, S. Nagata, Philos. Mag. B 71 (1995) 881.

[5] G. Oomi, T. Kagayama, I. Yoshida, T. Hagino, S. Nagata, J. Magn. Magn. Mater. 140-144 (1995) 157.

[6] T. Oda, M. Shirai, N. Suzuki, K. Motizuki, J. Phys.: Condens. Matter 7 (1995) 4433.

[7] K. Kumagai, S. Tsuji, T. Hagino, S. Nagata, in *Spectroscopy of Mott Insulators and Correlated Metals*, Springer Series in Solid-State Sciences, Vol. 119, edited by A. Fujimori, Y. Tokura (Springer-Verlag, Berlin, 1995), p.255.

[8] S. Nagata, S. Yasuzuka, Y. Kato, T. Hagino, M. Matsumoto, N. Kijima, S. Ebisu, Czech. J. of Phys 46 Suppl. S5, (1996) 2425.

[9] P. Somasundaram, J. M. Honig, T. M. Pekarek, B. C. Crooker, J. Appl. Phys 79 (1996) 5401.

[10] T. Furubayashi, T. Kosaka, J. Tang, T. Matsumoto, Y. Kato, S. Nagata, J. Phys. Soc. Jpn. 66 (1997) 1563.

[11] J. Matsuno, T. Mizokawa, A. Fujimori, D. A. Zatsepin, V. R. Galakhov, E. Z. Kurmaev, Y. Kato, S. Nagata, Phys. Rev. B 55 (1997) R15979.

[12] S. Tsuji, K. Kumagai, N. Matsumoto, Y. Kato, S. Nagata, Physica B 237-238 (1997) 156.

[13] S. Tsuji, K. Kumagai, N. Matsumoto, S. Nagata, Physica C 282-287 (1997) 1107.

[14] F. A. Chudnovskii, A. L. Pergament, G. B. Stefanovich, P. Somasundaram, J. M. Honig, Phys. Stat. Sol. (a) 162 (1997) 601.

[15] P. Somasundaram, D. Kim, J. M. Honig, T. M. Pekarek, J. Appl. Phys. 81 (1997) 4618.

[16] H. Kang, P. Mandal, I. V. Medvedeva, K. Bärner, A. Poddar, E. Gmelin, Phys. Stat. Sol. (a) 163 (1997) 465.

[17] E. Z. Kurmaev *et al.* Solid State Commun. 108 (1998) 235.

[18] S. Nagata, N. Matsumoto, Y. Kato, T. Furubayashi, T. Matsumoto, J. P. Sanchez, P. Vulliet, Phys. Rev. B 58 (1998) 6844.

[19] J. Tang, T. Matsumoto, T. Furubayashi, T. Kosaka, S. Nagata, Y. Kato, J. Magn. Magn. Mater. 177-181 (1998) 1363.

[20] J. Tang, T. Furubayashi, T. Kosaka, S. Nagata, Y. Kato, H. Asano, T. Matsumoto, Rev. High Pressure Sci. Technol. 7 (1998) 496.

[21] H. Kang, K. Bärner, I. V. Medvedeva, P. Mandal, A. Poddar, E. Gmelin, J. Alloys and Compounds 267 (1998) 1.

[22] P. Somasundaram, D. Kim, J. M. Honig, T. M. Pekarek, T. Gu, A. I. Goldman, J. Appl. Phys 83 (1998) 7243.

[23] H. Kang, P. Mandal, I. V. Medvedeva, J. Liebe, G. H. Rao, K. Bärner, A. Poddar, E. Gmelin, J. Appl. Phys. 83 (1998) 6977.

[24] K. Balcerek, Cz. Marucha, R. Wawryk, T. Tyc, N. Matsumoto, S. Nagata, Philos. Mag. B 79 (1999) 1021.

[25] N. Matsumoto, R. Endoh, S. Nagata, T. Furubayashi, T. Matsumoto, Phys. Rev. B 60 (1999) 5258.

[26] J. Tang, T. Matsumoto, T. Naka, T. Furubayashi, S. Nagata, N. Matsumoto, Physica B 259-261 (1999) 857.

[27] R. Oshima, H. Ishibashi, K. Tanioka, K. Nakahigashi, in *Proc. the Int. Conf. On Solid-Solid Phase Transformations '99 (JIMIC-3)*, edited by M. Koiwa, K. Otsuka, T. Miyazaki (The Japan Institute of Metals, 1999), p. 895.

[28] H. Suzuki, T. Furubayashi, G. Cao, H. Kitazawa, A. Kamimura, K. Hirata, T. Matsumoto, J. Phys. Soc. Jpn. 68 (1999) 2495.

[29] A. T. Burkov, T. Nakama, K. Shintani, K. Yagasaki, N. Matsumoto, S. Nagata, Phys. Rev. B 61 (2000) 10049.

[30] A. T. Burkov, T. Nakama, K. Shintani, K. Yagasaki, N. Matsumoto, S. Nagata, Physica B 281-282 (2000) 629.

[31] N. Matsumoto, S. Nagata, J. Crystal Growth 210 (2000) 772.

[32] M. Hayashi, M. Nakayama, T. Nanba, T. Matsumoto, J. Tang, S. Nagata, Physica B 281-282 (2000) 631.

[33] K. Kumagai, K. Kakuyanagi, R. Endoh, S. Nagata, Physica C 341-348 (2000) 741.

[34] Y. Kishimoto, T. Ohno, S. Nagata, N. Matsumoto, T. Kanashiro, Y. Michihiro, K. Nakamura, Physica C 281-282 (2000) 634.

[35] A. Goto, T. Shimizu, G. Cao, H. Suzuki, H. Kitazawa, T. Matsumoto, Physica C 341-348 (2000) 737.

[36] G. Cao, H. Suzuki, T. Furubayashi, H. Kitazawa, T. Matsumoto, Physica B 281-282 (2000) 636.

[37] G. L. W. Hart, W. E. Pickett, E. Z. Kurmaev, D. Hartmann, M. Neumann, A. Moewes, D. L. Ederer, R. Endoh, K. Taniguchi, S. Nagata, Phys. Rev. B 61 (2000) 4230.

[38] H. Kang, K. Bärner, H. Rager, U. Sondermann, P. Mandal, I. V. Medvedeva, E. Gmelin, J. Alloys and Compounds 306 (2000) 6.

[39] J. Tang, T. Kikekawa, J. Z. Hu, J. F. Shu, H. K. Mao, T. Furubayashi, A. Matsushita, T. Matsumoto, S. Nagata, N. Matsumoto, in *Proc. the Int. Conf. OnScience and Technology of High Pressure, (AIRAPT-17)*, edited by M. H. Manghnani, W. J. Nellis, M. F. Nicol, (2000), p.506.

[40] H. Ishibashi, T. Sakai, K. Nakahigashi, J. Magn. Magn. Mater. 226-230 (2001) 233.

[41] N. Matsumoto, Y. Yamauchi, J. Awaka, Y. Kamei, H. Takano, S. Nagata, Int. J. Inorg. Mater. 3, (2001) 791.

[42] W. Sun, T. Kimoto, T. Furubayashi, T. Matsumoto, S. Ikeda, S. Nagata, J. Phys. Soc. Jpn, 70 (2001) 2817.

[43] K. Oikawa, T. Matsumoto, T. Furubayashi, N. Matsumoto, S. Nagata, J. Phys. Soc. Jpn, 70 Suppl. (2001) A106.

[44] A. Goto, T. Shimizu, G. Cao, H. Suzuki, H. Kitazawa, T. Matsumoto, J. Phys. Soc. Jpn. 70 (2001) 9.

[45] R. Endoh, N. Matsumoto, S. Chikazawa, S. Nagata, T. Furubayashi, T. Matsumoto, Phys. Rev. B 64 (2001) 075106.

[46] G. Cao, T. Furubayashi, H. Suzuki, H. Kitazawa, T. Matsumoto, Y. Uwatoko, Phys. Rev. B 64 (2001) 214514.

[47] K. Yagasaki, T. Nakama, M. Hedo, A. T. Burkov, N. Matsumoto, S. Nagata, J. Magn. Magn. Mater. 226-230 (2001) 244.

[48] P. G. Radaelli, Y. Horibe, M. J. Gutmann, H. Ishibashi, C. H. Chen, R. M. Ibberson, Y. Koyama, Y-S. Hor, V. Kiryukhin, S-W. Cheong, Nature 416 (2002) 155.

[49] R. Endoh, N. Matsumoto, J. Awaka, S. Ebisu, S. Nagata, J. Phys. Chem. Solids 63 (2002) 669.

[50] K. Yagasaki, T. Nakama, M. Hedo, K. Uchima, Y. Shimoji, N. Matsumoto, S. Nagata, H. Okada, H. Fujii, A. T. Burkov, J. Phys. Chem. Solids 63 (2002) 1051.

[51] S. Nagata, S. Ito, R. Endoh, J. Awaka, Philos. Mag. B 82 (2002) 1679.

[52] H. Ishibashi, T. Y. Koo, Y. S. Hor, A. Borissov, P. G. Radaelli, Y. Horibe, S. W. Cheong, V. Kiryukhin, Phys. Rev. B 66 (2002) 144424.

[53] V. N. Andreev, F. A., Chudnovskiy, S. Perooly, J. M. Honig, Phys. Stat. Sol. (b) 234 (2002) 623.

[54] S. Nagata, N. Matsumoto, R. Endoh, N. Wada, Physica B 329-333 (2003) 944.

[55] T. Furubayashi, H. Suzuki, T. Matsumoto, S. Nagata, Solid State Commun. 126 (2003) 617.

[56] M. Croft, W. Caliebe, H. Woo, T. A. Tyson, D. Sills, Y. S. Hor, S-W. Cheong, V. Kiryukhin, S-J. Oh, Phys. Rev. B 67 (2003) 201102.

[57] R. Endoh, J. Awaka, S. Nagata, Phys. Rev. B 68 (2003) 115106.

[58] K. Kitamoto, Y. Taguchi, K. Miura, K. Ichikawa, O. Aita, H. Ishibashi, Phys. Rev. B 68 (2003) 195124.

[59] M. Yamamoto, S. Noguchi, H. Ishibashi, T. Ishida, Physica 329-333B (2003) 940.

[60] K. Betsuyaku, H. Ishibashi, A. Yanase, N. Hamada, J. Magn. Magn. Mater. 272-276 (2004) e295.

[61] T. Furubayashi, H. Suzuki,T. Matsumoto, S. Nagata, J. Magn. Magn. Mater 272-276 (2004) 446.

[62] T. Okane, S.-i. Fujimori, K. Mamiya, J. Okamoto, Y. Muramatsu, A. Fujimori, H. Suzuki, T. Matsumoto, T. Furubayashi, M. Isobe, S. Nagata, J. Magn. Magn. Mater. 272-276 (2004) e297.

[63] S. Nagata, T. Asakura, J. Awaka, J. Magn. Magn. Mater. 272-276 (2004) 392.

[64] T. Sasaki, M. Arai, T. Furubayashi, T. Matsumoto, J. Phys. Soc. Jpn. 73 (2004) 1875.

[65] M. Sasaki, K. Kumagai, K. Kakuyanagi, S. Nagata, Physica C 408-410 (2004) 822.

[66] L. Chen, M. Matsunami, T. Nanba, T. Matsumoto, S. Nagata, Y. Ikemoto, T. Moriwaki, T. Hirono, H. Kimura, J. Phys. Soc. Jpn. 74 (2005) 1099.

[67] S. Nagata, Chinese J. Phys. 43 (2005) No. 3-II, 722.

[68] D. I. Khomskii, T. Mizokawa, Phys. Rev. Lett. 94 (2005) 156402.

[69] K. Takubo, S. Hirata, J.-Y. Son, J. W. Quilty, T. Mizokawa, N. Matsumoto, S. Nagata, Phys. Rev. Lett. 95 (2005) 246401.

[70] R. M. Fleming, F. J. DiSalvo, R. J. Cava, J. V. Waszczak, Phys. Rev. B 24 (1981) 2850.

[71] F. J. DiSalvo, J. V. Waszczak, Phys. Rev. B 26 (1982) 2501.

[72] T. Sekine, K. Uchinokura, H. Iimura, R. Yoshizaki, E. Matsuura, Solid State Commun. 51 (1984) 187.

[73] J. Mahy, D. Colaitis, D. Van Dyck, S. Amelinckx, J. Sold State Chem. 68 (1987) 320.

[74] T. Hagino, Y. Seki, S. Takayanagi, N. Wada, S. Nagata, Phys. Rev. B 49 (1994) 6822.

[75] Y. Kishimoto, T. Ohno, T. Kanashino, Y. Michihiro, K. Mizuno, M. Miyamoto, T. Tanaka, K. Miyatani, Solid State Commun. 96 (1995) 23.

[76] Z. W. Lu, B. M. Klein, E. Z. Kurmaev, V. M. Cherkashenko, V. R. Galakhov, S. N. Shamin, Yu. M. Yarmoshenko, V. A. Trofimova, St. Uhlenbrock, M. Neumann, T. Furubayashi, T. Hagino, S. Nagata, Phys. Rev. B 53 (1996) 9626.

[77] Y. Yoshikawa, S. Wada, K. Miyatani, T. Tanaka, M. Miyamoto, Phys. Rev. B 55 (1997) 74.

[78] T. Tanaka, K. Miyatani, J. Phys. Soc. Jpn. 66 (1997) 3341.

[79] J. Matsuno, A. Fujimori, L. F. Mattheiss, R. Endoh, S. Nagata, Phys. Rev. B 64 (2001) 115116.

[80] H. Chudo, H. Nakamura, M. Shiga, Solid State Commun. 129 (2004) 677.

[81] H. Okada, K. Koyama, K. Watanabe, J. Phys. Soc. Jpn. 73 (2004) 3227.

[82] R. Burrell, D. M. Klementowicz, F. M. Groshe, J. Awaka, S. Nagata, Physica B 359-361 (2005) 1201.

[83] D.A. Crandles, M. Reedyk, G. Wardlaw, F. S. Razavi, T. Hagino, S. Nagata, I. Shimono, R. K. Kremer, J. of Phys.: Condens. Matter, 17 (2005) 4813.